Excited-State Structures

DOI: 10.1002/anie.200900741

Structural Tracking of a Bimolecular Reaction in Solution by Time-Resolved X-Ray Scattering**

Kristoffer Haldrup, Morten Christensen, Marco Cammarata, Qingyu Kong, Michael Wulff, Simon O. Mariager, Klaus Bechgaard, Robert Feidenhans'l, Niels Harrit, and Martin M. Nielsen**

Every photochemical reaction starts with an electronically excited state and ends with a ground-state molecule. This is also true in bimolecular photoreactions, in which the excited molecule collides with a ground-state reactant. The collision complex may follow a potential energy surface directly to the primary ground-state product. The reaction may also proceed on an excited-state surface and reach a stable minimum configuration. This excited complex—an exciplex—is anticipated to precede the primary product of many types of bimolecular photoreactions, most prominently in photoinduced electron-transfer reactions.[1]

The presence of an exciplex is easily demonstrated if it emits a characteristic emission. However, this situation is the exception rather than the rule, and exciplexes are generally not easily detected. An alternative to emission spectroscopy is time-resolved absorption spectroscopy based on laser methods. Unfortunately, neither type of spectroscopy provides direct structural information. The present study presents time-resolved X-ray scattering in aqueous solution as a new means of directly obtaining a model-independent structure of this kind of elusive intermediate.

The advent of intense and pulsed X-ray beams from synchrotron insertion devices has opened up unprecedented opportunities to obtain structural information on transient molecules.[2,3] In the crystalline state, diffraction studies have allowed structure determination of photoexcited molecules[4–7] including the $^3A_{2u}$ state of salts of octahydrogen[tetrakis-μ-diphosphito-1κ*P*:2κ*P*′-diplatinate](4-) (PtPOP*)[5,6] and excimers.[8] Only recently have time-resolved scattering studies of reactions in solutions become possible despite the large background scattering from the solvent[9] and the absence of signal amplification from long-range order. The theoretical foundation of the laser/X-ray pump–probe method has been established,[10,11] and the solvent response to impulsive heating has been described.[12,13] Thus, solution-state pump–probe X-ray scattering studies on time scales of picoseconds to nanoseconds have been reported[14] for light-induced reactions of small molecules such as I_2, HgI_2, CH_2I_2, and $C_2H_4I_2$[15,16] dissolved in CCl_4 and methanol, and for gold nanoparticles in water.[17] The excited $^3A_{2u}$ state of PtPOP* represents the most complex structure hitherto investigated in solution by time-resolved X-ray scattering.[18]

PtPOP* displays characteristic photophysical (phosphorescence quantum yield, $\Phi_p = 0.5$; lifetime, $\tau_p = 10\ \mu s$[19,20]) and photochemical properties. Hydrogen/halogen atom abstraction and photocatalytical generation of H_2 by C–H bond cleavage are among the reactions reported.[21] PtPOP* also forms excited-state complexes (exciplexes) with, for example, Tl^+ ions. This bimolecular reaction is of particular interest as it was the first metal–metal bonded exciplex formation to be reported.[22–24]

The present study deals with the exciplex TlPtPOP*, which forms between PtPOP* and a single Tl^+ ion, in the time frame from 100 ps to 100 ns after excitation. The processes occurring are illustrated in Figure 1. On longer time scales, or at high concentrations of Tl^+ ions, an additional Tl^+ ion can combine with TlPtPOP* to form Tl_2PtPOP*.[24]

The liquid-scattering experiments were carried out on beamline ID09B at the ESRF facility following a well-established laser/X-ray pump–probe protocol.[9,18,25] The concentrations in a typical experiment were [PtPOP] = 12 mM and [Tl^+] = 7.2 mM. The aqueous solution was circulated under oxygen-free conditions through a sapphire nozzle producing a 0.3 mm thick sheet of liquid. This was crossed by the laser and X-ray beams. The optical pump pulse at 390 nm was generated by frequency doubling the 780 nm output of a Ti:sapphire laser. To reduce multiphoton excitation of the solvent as well as other higher-order effects, the peak intensity of the pump pulse was reduced by stretching the 150 fs pulse to 2 ps.

The X-ray probe pulse was created by an undulator insertion device producing a "pink-beam" energy profile with a maximum at 18.2 keV and 3% bandwidth after passing the X-ray optics. The X-rays from a single bunch in the storage

[*] Dr. K. Haldrup, M. Christensen, S. O. Mariager, Prof. K. Bechgaard, Prof. R. Feidenhans'l, Prof. N. Harrit, Prof. M. M. Nielsen
Centre for Molecular Movies, Department of Chemistry and Niels Bohr Institute, University of Copenhagen
Universitetsparken 5, 2100 Copenhagen (Denmark)
Fax: (+45) 3532-0460
E-mail: harrit@nano.ku.dk
meedom@nbi.dk

Dr. M. Cammarata, Dr. Q. Kong,[+] Prof. M. Wulff
European Synchrotron Radiation Facility, Grenoble Cedex 38043 (France)

[+] Current address:
Société Civile Synchrotron SOLEIL, Gif-sur-Yvette Cedex 9112 (France)

[**] The expert assistance provided by E. Pontecorvo and F. Ewald at the ID09B Beamline at ESRF, Grenoble, is very much appreciated. This work was supported by the Danish National Research Foundation's Centre for Molecular Movies and DANSCATT.

Supporting information for this article is available on the WWW under http://dx.doi.org/10.1002/anie.200900741.

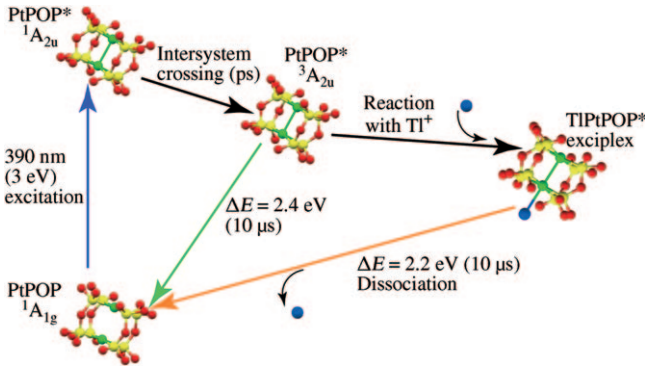

Figure 1. Simplified illustration of the photochemistry of Tl^+/PtPOP in aqueous solution. A laser pulse (2 ps, 390 nm) excites PtPOP in aqueous solution from the $^1A_{1g}$ ground state to the $^1A_{2u}$ excited state. Rapid (ps) intersystem crossing transforms the molecule into the $^3A_{2u}$ state (PtPOP*), which in a bimolecular reaction can combine with a Tl^+ ion to form an exciplex. All excited-state molecules subsequently return radiatively or nonradiatively to the ground state on a μs time scale. Concomitantly, the exciplex dissociates. Energy values were taken from Clodfelter et al.[24] Color code: Pt green, Tl blue, O red, P yellow; H is omitted for clarity.

ring were isolated by a high-speed chopper[14] operating in phase with the pulse repetition frequency of the pump laser. The temporal resolution of the setup depends on the bunch structure of the storage ring, but it was always better than 100 ps and can approach 50 ps. Timing jitter was 3–5 ps.[15] Six time delays (Δt) between the pump and probe pulses were investigated in the range from 100 ps to 25 ns.

The scattered X-rays were detected by an integrating area detector placed 50 mm from the sample, allowing photons with scattering angles up to $2\theta = 55°$ to be collected. The integration time was 10 s, corresponding to 9863 individual pump–probe events. As in similar pump–probe studies,[9,13] the data were acquired in an alternating sequence of laser-on/laser-off images to minimize effects of system drift.

The two-dimensional scattering patterns were converted to one-dimensional radial curves $S(2\theta)$. Difference curves $\Delta S(2\theta,\tau)$ were obtained by subtracting the average of two neighboring laser-off curves from the laser-on curve between them. The ratio $\Delta S/S$ for the PtPOP system under investigation here is typically below 10^{-3}, underlining the need for careful scaling and averaging. The $\Delta S(2\theta)$ curves were converted to $\Delta S(Q)$, $Q = \frac{4\pi}{\lambda}\sin\theta$, using the spectral profile $I(\lambda)$ of the X-ray beam.

Figure 2 A shows $Q\Delta S(Q)$ curves for three representative time delays, $\Delta t = 100$ ps, 2 ns, and 25 ns. In these curves, three distinct Q regions are apparent for all time steps: 1) A low-Q part below $Q = 1$ Å^{-1} exhibiting a distinct increase as time progresses, 2) an intermediate range from $Q = 1$ to $Q = 4$ dominated by a single large oscillation, and 3) a high-Q part beyond $Q = 4$ showing oscillations that shift slightly as the time delay between the pump and the probe is increased from 100 ps to 25 ns.

The scattered forward intensity ($Q = 0$) is proportional to the square of the number of electrons in the molecule.[26] Hence, for each exciplex being formed, the forward scattering signal will change by an amount proportional to $(Z_{PtPOP} + Z_{Tl})^2 - (Z_{PtPOP}{}^2 + Z_{Tl}{}^2) = 2Z_{PtPOP}Z_{Tl}$. The observation of a growin at low Q as the time delay increases from 100 ps to 25 ns

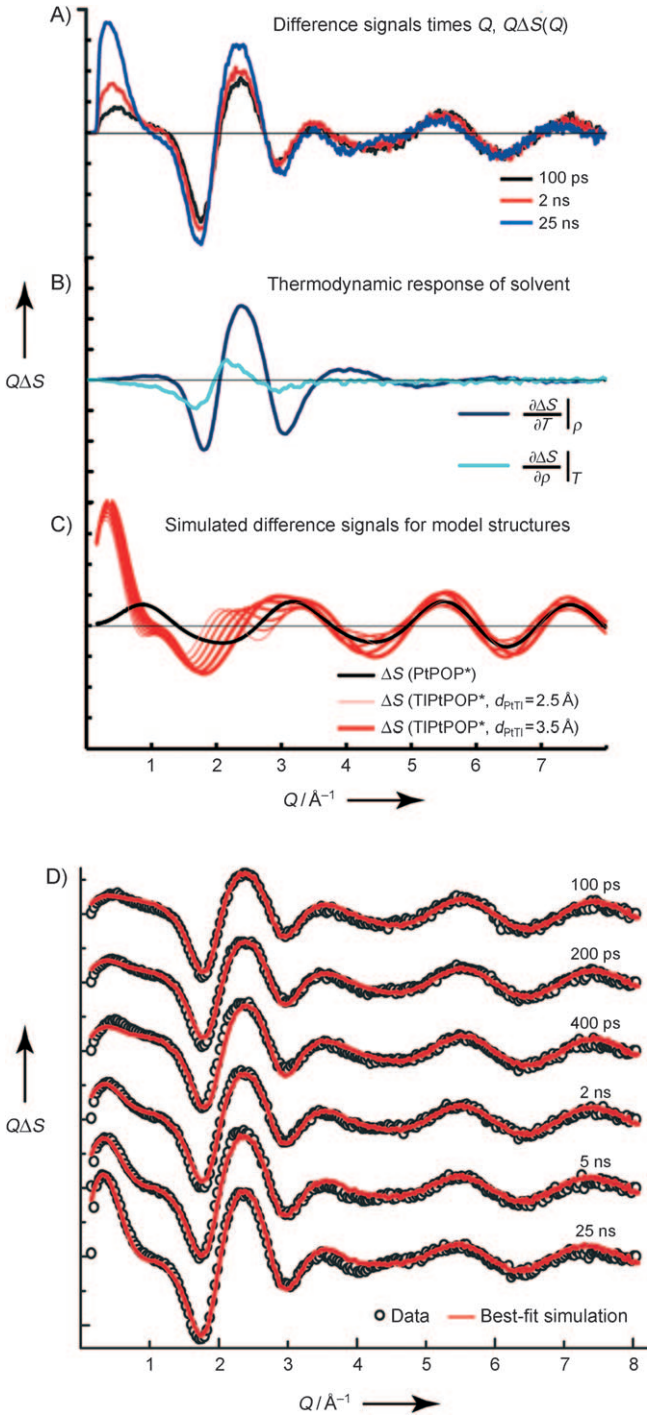

Figure 2. Experimental results and simulated data. A) Difference scattering signal (multiplied by Q) for three time delays: $\Delta t = 100$ ps, 2 ns, and 25 ns. B) Thermodynamic differentials,[13] $\frac{\partial(\Delta S)}{\partial T}\Big|_\rho$ and $\frac{\partial(\Delta S)}{\partial \rho}\Big|_T$, describing the solvent's thermodynamic response to impulse heating of 0.3 °C and density changes. C) Simulated scattering signals from PtPOP* (black) and from a range of putative exciplex structures each with a Pt–Tl distance of $d_{PtTl} = 2.5$–3.5 Å (red). D) Experimental data (black circles) and model fit (red lines) for the six time delays investigated ([PtPOP] = 12 mM, $[Tl^+]$ = 7.2 mM). For clarity, traces are off-set vertically.

constitutes unambiguous and model-independent proof that an associative reaction takes place.

In the intermediate Q range, the single large oscillation observed in this region is known from previous studies[13,27] to be a consequence of the thermodynamic response of the solvent, water, to the energy release associated with the fast intersystem crossing between the $^1A_{2u}$ and $^3A_{2u}$ states as shown in Figure 1. The contribution to the difference signal can be well described[13] by a linear combination of two thermodynamic differentials, $\Delta S_{\mathrm{solvent}} = \Delta T \frac{\partial(\Delta S)}{\partial T}\Big|_{\rho} + \Delta\rho \frac{\partial(\Delta S)}{\partial \rho}\Big|_{T}$. Figure 2B shows how the scattering signal is affected by changes in the solvent temperature and density.

The $Q > 3$ part of the difference scattering signals (Figure 2A) reflects a change in the configuration of coherently scattering electrons between $\Delta t = 100$ ps and $\Delta t = 25$ ns.

To explore how the scattering curve changes when the distance d_{PtTl} between the axially coordinated Tl and Pt atoms in TlPtPOP* is varied, $\Delta S_{\mathrm{TlPtPOP*}}(d_{\mathrm{PtTl}})$ was calculated as the Tl–Pt distance was increased from 2.5 Å to 3.5 Å in steps of 0.025 Å. The structure of PtPOP* was fixed using the atomic coordinates obtained in an independent time-resolved scattering study.[18] Since Pt and Tl have a comparable number of electrons, a possible change in the Pt–Pt distance will be too strongly correlated with the Pt–Tl distance for these values to be independently optimized when the calculated signal is fit to the measured.

Six of these curves are shown in Figure 2C, corresponding to increments of 0.2 Å in d_{PtTl} between each curve. In these simulations the fraction of excited states relative to ground-state PtPOP molecules, α, was provisionally fixed at $\alpha = 0.05$.[18] A fraction $\beta = 0.5$ of the excited states was assumed to have associated with Tl^+ to form TlPtPOP* exciplexes.

The determination of the Pt–Tl distance in the TlPtPOP* exciplex and of the time-dependent concentrations of the two excited-state species are dealt with quantitatively by expressing the total signal for any time delay, Δt, as the sum of the four terms in Equation (1).

$$\Delta S(Q)_{\mathrm{sim}} = \alpha \Delta S_{\mathrm{PtPOP*}} + \beta \Delta S_{\mathrm{TlPtPOP*}}(d_{\mathrm{PtTl}}) + \Delta T \frac{\partial(\Delta S)}{\partial T}\Big|_{\rho} + \Delta\rho \frac{\partial(\Delta S)}{\partial \rho}\Big|_{T} \quad (1)$$

The objective was to find the combinations of the five variable parameters (α, β, d_{PtTl}, ΔT, and $\Delta\rho$) (Table 1) that most accurately fit the difference signals. The search for a global best fit of structural models to the data was undertaken within a multiparameter maximum likelihood analysis (MLA) framework. The study employed a χ^2 estimator with χ^2 given by Equation (2).

$$\chi^2(d_{\mathrm{PtTl}}, \alpha, \beta, \Delta T, \Delta\rho) = \sum_{Q} \frac{(S_{\mathrm{sim}}(Q) - S_{\mathrm{data}}(Q))^2}{2\sigma_{\mathrm{Q}}^2} \Big/ (N - p - 1) \quad (2)$$

Here σ_{Q} is the standard deviation evaluated at each Q point, N is the number of Q points, and p the number of free parameters, for the goodness-of-fit for each combination of the five parameters.[28] Figure 2D illustrates the result of applying this method to the difference curves for every time delay, Δt, with the data shown as black circles and the best-fit scattering signal as red lines. For all time delays, good agreement is observed between the data and the simulations.

The approach is illustrated with reference to Figure 3, where the procedure is applied to the data set obtained for $\Delta t = 25$ ns. Within the framework of MLA, a (relative) likelihood can be assigned to each combination of the five fitting parameters through $L(\alpha, \beta, d_{\mathrm{PtTl}}, \Delta T, \text{ and } \Delta\rho) \propto \exp(-\chi^2)$.[28] Thus, correlations between the individual fitting parameters can be explored as shown in Figure 3A, where iso-likelihood curves are given for projections of the five-dimensional parameter space onto the four planes containing the d_{PtTl} distance as one axis. Correlations are observed between d_{PtTl} and the α and β parameters, which signify the strong connection between the amount of each individual molecular species and the height and shape of the $\Delta S(Q)$-curve oscillations.

To directly gauge the most-probable parameter value, without assuming any a priori knowledge of the other fitting parameters, the full five-dimensional likelihood distribution for the $\Delta t = 25$ ns data set was projected onto the d_{PtTl} axis, as shown in Figure 3B. From this, the most probable value of d_{PtTl} is determined to be 2.93 ± 0.12 Å, with the limits enclosing 68% of the total likelihood distribution.

Applying the projection method to the remaining parameters, a photoexcitation fraction of 3.9% was found to be most likely. Of this fraction, 55% has formed the exciplex at 25 ns, corresponding to a total concentration of TlPtPOP* ≈ 0.26 mM (Table 1). This value is in good agreement with the kinetic scheme and rate constants determined in earlier spectroscopic studies.[24]

No change in solvent density appears up to 25 ns, at which point the temperature rise is determined to be 0.3–0.4 °C. This increase is larger than expected from the observed excitation fraction (only 0.8 eV is released from intersystem crossing between the $^1A_{2u}$ and $^3A_{2u}$ states) and indicates the presence of nonlinear multiphoton processes such as re-excitation of $^1A_{2u}$ and $^3A_{2u}$.

To determine d_{PtTl} more accurately, two other experiments were carried out with concentrations of Tl^+ ions of 3.4 mM and 1.8 mM, respectively. All other conditions were unchanged. Selected data from all three series are collected in Table 1. For

Table 1: Optimized fitting parameters for three experimental series with [PtPOP] = 12 mM and Tl^+ concentrations as indicated in the first column. For each, the time delay Δt with the highest concentration of the TlPtPOP* exciplex is presented. Parameters α, β, d_{PtTl}, ΔT, and $\Delta\rho$ are defined in the text [see Eq. (1)].

$[Tl^+]$ [mM]	Δt [ns]	α	β	$[\mathrm{PtPOP*}]_{\mathrm{max}}$ [mM]	$[\mathrm{TlPtPOP*}]_{\mathrm{max}}$ [mM]	d_{PtTl} [Å]	ΔT [K]	$\Delta\rho$ [kg m^{-3}]
7.2	25	0.039 (±0.015)	0.55 (±0.19)	0.47 (±0.18)	0.26 (±0.09)	2.93 (±0.12)	0.36 (±0.08)	0.01 (±0.07)
3.4	100	0.027 (±0.013)	0.49 (±0.22)	0.32 (±0.16)	0.16 (±0.07)	2.93 (±0.17)	0.30 (±0.07)	-0.08 (±0.06)
1.8	100	0.019 (±0.013)	0.33 (±0.25)	0.23 (±0.16)	0.08 (±0.06)	2.88 (±0.29)	0.17 (±0.08)	-0.01 (±0.07)

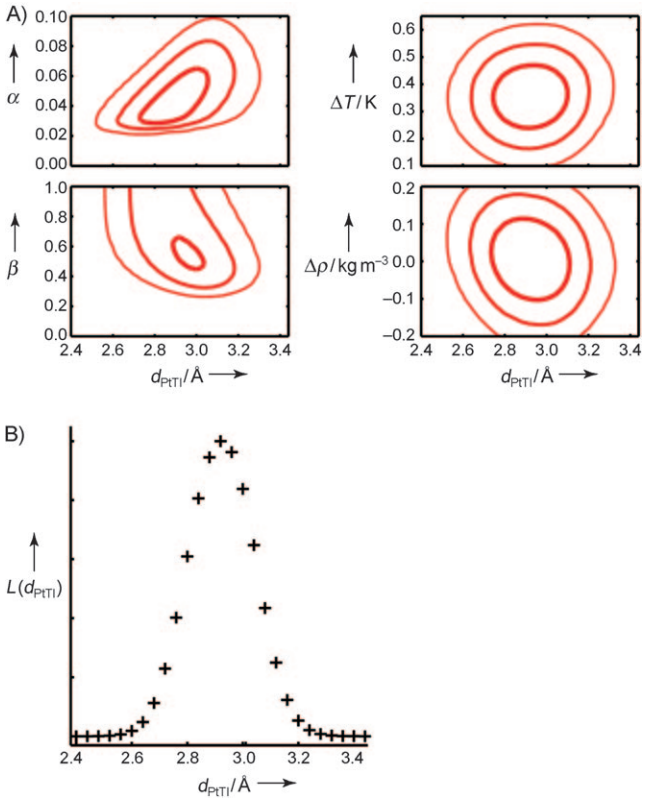

Figure 3. Fitting procedure for the $\tau = 25$ ns data set ([PtPOP] = 12 mM, [Tl^+] = 7.2 mM). A) Two-dimensional likelihood-distribution plots showing the strong correlation between d_{PtTl} and the (relative) fractions of the excited-state species PtPOP* and TlPtPOP*. Contours enclose (from thick to thin) 68.3%, 95.4% and 99.8%, respectively, of the total likelihood distribution. B) Normalized likelihood distribution as function of d_{PtTl} only. A clear maximum is observed for $d_{PtTl} = 2.93$ Å.

each series, the time delay (Δt) with the highest concentration of the TlPtPOP* exciplex is presented. The five fitting parameters and their optimal values are listed. In addition to the relative fractions of excitation (α) of PtPOP and the maximum fraction exciplex formed (β), the corresponding concentrations $[PtPOP^*]_{max}$ and $[TlPtPOP^*]_{max}$ have also been calculated, as these provide a means for understanding the differences in the error estimates. For the lower Tl^+ concentrations, the optimum exciplex concentration was found at longer time delays in accordance with the kinetics of exciplex formation. The uncertainty in the determination of d_{PtTl} is observed to increase with decreasing exciplex concentration, as would be expected.

Combining the results for the three time delays with the highest concentrations of TlPtPOP*, the value $d_{PtTl} = 2.92 \pm 0.09$ Å was obtained. The Tl–Pt distance, $d_{PtTl} = 2.92 \pm 0.09$ Å, thus derived for TlPtPOP*, is in good agreement with previous estimates of 2.7 to 3.0 Å,[24] but it is considerably shorter than the distance reported for the structurally similar system $[Tl_2Pt(CN)_4]$ ($d_{PtTl} = 3.14$ Å, crystal data[29]). However, it is in good agreement with the value $d_{PtTl} = 2.88$ Å predicted in a calculation of the structure of $[Tl_2Pt(CN)_4]$ in vacuum.[24]

Time-resolved X-ray scattering measurements directly provide structural information about excited states and other short-lived species. The present study demonstrates how this method can be extended to bimolecular reactions occurring on very short time scales in solution.

Experimental Section

The Supporting Information contains: 1) experimental procedures pertaining to sample handling, 2) a description of the actual liquid jet used together with a description of beamline ID-09B at ESRF, and 3) extensive accounts of the data analysis.

Received: February 6, 2009
Published online: April 29, 2009

Keywords: exciplexes · photochemistry · platinum · X-ray scattering

[1] G. J. Kavarnos, *Fundamentals of Photoinduced Electron Transfer*, Wiley-VCH, New York, **2008**.
[2] D. J. Thiel, P. Livins, E. A. Stern, A. Lewis, *Nature* **1993**, *362*, 40–43.
[3] L. X. Chen, W. J. H. Jager, G. Jennings, D. J. Gosztola, A. Munkholm, J. P. Hessler, *Science* **2001**, *292*, 262–264.
[4] S. Techert, F. Schotte, M. Wulff, *Phys. Rev. Lett.* **2001**, *86*, 2030–2033.
[5] C. D. Kim, S. Pillet, G. Wu, W. K. Fullagar, P. Coppens, *Acta Crystallogr. Sect. A* **2002**, *58*, 133–137.
[6] N. Yasuda, H. Uekusa, Y. Ohashi, *Bull. Chem. Soc. Jpn.* **2004**, *77*, 933–944.
[7] F. Schotte, M. Lim, T. A. Jackson, A. V. Smirnov, J. Soman, J. S. Olson, G. N. Phillips, Jr., M. Wulff, P. A. Anfinrud, *Science* **2003**, *300*, 1944–1947.
[8] I. I. Vorontsov, A. Y. Kovalevsky, Y. S. Chen, T. Graber, M. Gembicky, I. V. Novozhilova, M. A. Omary, P. Coppens, *Phys. Rev. Lett.* **2005**, *94*, 193003.
[9] H. Ihee, M. Lorenc, T. K. Kim, Q. Y. Kong, M. Cammarata, J. H. Lee, S. Bratos, M. Wulff, *Science* **2005**, *309*, 1223–1227.
[10] S. Bratos, F. Mirloup, R. Vuilleumier, M. Wulff, *J. Chem. Phys.* **2002**, *116*, 10615–10625.
[11] N. E. Henriksen, K. B. Moller, *J. Phys. Chem. B* **2008**, *112*, 558–567.
[12] P. Georgiou, J. Vincent, M. Andersson, A. B. Wohri, P. Gourdon, J. Poulsen, J. Davidsson, R. Neutze, *J. Chem. Phys.* **2006**, *124*, 234507.
[13] M. Cammarata, M. Lorenc, T. K. Kim, J. H. Lee, Q. Y. Kong, E. Pontecorvo, M. Lo Russo, G. Schiro, A. Cupane, M. Wulff, H. Ihee, *J. Chem. Phys.* **2006**, *124*, 124504.
[14] M. Wulff, A. Plech, L. Eybert, R. Randler, F. Schotte, P. Anfinrud, *Faraday Discuss.* **2002**, *122*, 13–26.
[15] R. Neutze, R. Wouts, S. Techert, J. Davidsson, M. Kocsis, A. Kirrander, F. Schotte, M. Wulff, *Phys. Rev. Lett.* **2001**, *87*, 195508.
[16] M. Wulff, S. Bratos, A. Plech, R. Vuilleumier, F. Mirloup, M. Lorenc, Q. Kong, H. Ihee, *J. Chem. Phys.* **2006**, *124*, 034501.
[17] A. Plech, V. Kotaidis, K. Istomin, M. Wulff, *J. Synchrotron Radiat.* **2007**, *14*, 288–294.
[18] M. Christensen, K. Haldrup, K. Bechgaard, R. Feidenhans'l, Q. Kong, M. Cammarata, M. Russo, M. Wulff, N. Harrit, M. Nielsen, *J. Am. Chem. Soc.* **2009**, *131*, 502–508.
[19] C. M. Che, L. G. Butler, H. B. Gray, *J. Am. Chem. Soc.* **1981**, *103*, 7796–7797.
[20] A. E. Stiegman, S. F. Rice, H. B. Gray, V. M. Miskowski, *Inorg. Chem.* **1987**, *26*, 1112–1116.
[21] D. M. Roundhill, H. B. Gray, C. M. Che, *Acc. Chem. Res.* **1989**, *22*, 55–61.

[22] J. K. Nagle, B. A. Brennan, *J. Am. Chem. Soc.* **1988**, *110*, 5931 – 5932.
[23] M. S. Herman, J. L. Goodman, *J. Am. Chem. Soc.* **1989**, *111*, 9105 – 9107.
[24] S. A. Clodfelter, T. M. Doede, B. A. Brennan, J. K. Nagle, D. P. Bender, W. A. Turner, P. M. LaPunzina, *J. Am. Chem. Soc.* **1994**, *116*, 11379 – 11386.
[25] M. Wulff, A. Plech, L. Eybert, R. Randler, F. Schotte, P. Anfinrud, *Faraday Discuss.* **2003**, *122*, 13 – 26.
[26] J. Als-Nielsen, D. McMorrow, *Elements of Modern X-ray Physics*, Wiley, Chichester, **2000**, p. 112.
[27] A. Plech, V. Kotaidis, M. Lorenc, M. Wulff, *Chem. Phys. Lett.* **2005**, *401*, 565 – 569.
[28] W. H. Press, B. P. Flannery, T. A. Teukolsky, W. T. Vetterling, *Numerical Recipes—The Art of Scientific Computing*, Cambridge University Press, Cambridge, **1986**.
[29] M. Maliarik, J. K. Nagle, A. Ilyukhin, E. Murashova, J. Mink, M. Skripkin, O. J. Glaser, M. Kovacs, A. Horvath, *Inorg. Chem.* **2007**, *46*, 4642 – 4653.

